Vacuum-free synthesis of water-based CZTS ink for optoelectronics applications

H. GULUPALLI[1,2], I. SHARMA[1], B. LOKESH[1], K. BORSE[1,*]
[1]*Department of Metallurgical and Materials Engineering, Malaviya National Institute of Technology Jaipur, Jaipur, Rajasthan, 302017, India*
[2]*Department of Materials Science and Engineering, Cornell University, Ithaca, NY 14850, United States of America*

The present work demonstrates a novel low-temperature vacuum-free synthesis of water-based printable CZTS (Cu_2ZnSnS_4) semiconductor ink. Various sophisticated characterization techniques, such as X-ray diffraction and Raman spectroscopy, confirmed the presence of the CZTS in the ink. Ultraviolent-visible spectroscopy showed the bandgap of the CZTS ink to be 1.5 eV, calculated using the Tauc plot method, while the particle size analysis, viscosity, and hydrophilic nature of the prepared ink confirmed its suitability for ink-jet printing. This endeavor will facilitate the development of a simple, affordable technique for the ongoing improvement of CZTS ink.

(Received October 14, 2024; accepted April 3, 2025)

Keywords: CZTS, Semiconductor ink, XRD, Tauc plot, Particle size analysis, Raman Spectroscopy

1. Introduction

The need to discover renewable energy sources becomes prominent to achieve sustainable development, reduce carbon footprint, and reduce our reliance on conventional energy sources [1, 2]. In recent years, second-generation semiconductors like Cu_2ZnSnS_4 (CZTS) have been gaining a lot of attention to be used as a photo-absorbing material in the field of solar photovoltaic technology and have become an excellent contender in the category of thin films based on solar cells [3-7]. Unfortunately, the limited availability of the constituent elements and toxicity are a few of the major bottlenecks of other CZTS counterparts in the thin film solar cells category [3, 8]. With the presence of plentiful and innocuous constituent elements such as Cu, Zn, Sn, and S, high absorption coefficient, and tunable band gap, depending on the composition, CZTS becomes an ideal and most promising candidate for the optoelectronic application as a photo-absorbing material. For the Cu_2ZnSnS_4 (CZTS) based thin film solar cells, with initial power conversion efficiency (PCE) of ~ 3%, a maximum of 12.3% PCE is recently reported by alloying the CZTS with cadmium [9-11]. In other ways, such as heterojunction heat treatment followed by sulphurization, a PCE crossing 10% has been achieved [12]. Although CZTS solar cells have demonstrated their promise, the cost and complexity involved in their synthesis still remain a challenge [13-15].

The CZTS thin film can be prepared by using two major techniques, viz. vacuum-based techniques and non-vacuum-based techniques. A few of the vacuum-based methods are electron beam evaporation and sulfurization, pulsed laser deposition technique (PLD), and sputtering techniques [16-18]. These vacuum-based techniques increase the high cost of manufacturing while making the large area deposition a problematic task. On the other hand, non-vacuum-based methods include spray pyrolysis techniques, electrochemical deposition techniques, and sol-gel deposition techniques [19-23]. These non-vacuum methods are reasonably economical and industrially scalable; however, there are some disadvantages, including the involvement of high temperatures exceeding 200 ºC, a necessity for multiple steps, and the use of incredibly complicated and intricate techniques to coat the substrate. Table 1 provides a concise overview of CZTS-based solar cells, with respect to the solar cell structure, the deposition/ synthesis technique of CZTS absorbing film, and the respective power conversion efficiency achieved.

In non-vacuum-based techniques, ink-jet printing can be thought of as an industrially viable method that can be used for large-area solar cell fabrication. This method requires the availability of semiconductor ink to be deposited as a photo-absorbing material. Therefore, the present work involves the single-stage synthesis of CZTS ink, which is possible at relatively very low temperatures in an open atmosphere and can be easily processed via inkjet printing.

Table 1. Summarization of CZTS-based solar cell synthesis technique and efficiency

S. No	Device Structure	CZTS Deposition/Synthesis Technique	PCE Achieved	References
1	Glass/Mo/CZTS/Graphene/CdS/ZnO/AZO/Al	RF Magnetron sputtering	7.59%	[24]
2	Ti/ Mo/ CZTS/ CdS/ TCO/ Ag	Spincoating followed by annealing at 300 ºC and subsequent sulphurization	6.94%	[25]
3	Mo/ CZTS/ ZnSnO/ ZnO/ ITO	Co-sputtering	11%	[26]
4	Mo/CZTS/ZnSnO/ZnO/ITO/Ni-Al-Ni/MgF2	Sputtering	11.40%	[27]
5	Glass/ Mo/ CZTS/ CDS/ ZnO:Ga/Al	RF magnetron sputtering	7.60%	[28]

2. Experimental

Unless precisely specified, all activities were performed in the air. Copper (II) sulfate pentahydrate ($CuSO_4.5H_2O$) (99.99%), Zinc sulfate heptahydrate ($ZnSO_4.7H_2O$) (98%), Stannous sulphate ($SnSO_4$) (98%) and Thiourea (CH_4N_2S), Hydrazine hydrate ($NH_2NH_2 \cdot H_2O$) (80% solution in water) were purchased from Sigma Aldrich and used as received without any further purification.

At first, Chemicals/ constituents of CZTS such Copper (II) sulfate pentahydrate (0.5 M), Zinc sulfate heptahydrate, (0.25 M), Stannous sulphate, (0.25 M) and Thiourea, (1.00 M) were dissolved in a proportion of 2:1:1:4 respectively in DI water, according to the chemical formula of CZTS (Cu_2ZnSnS_4). Using magnetic stirring, the solution was allowed to stir at room temperature for ~ 1 hour to get a blue colored homogenous solution, followed by increasing the temperature to 45 ºC and adding strong reducing agent hydrazine hydrate (5 M) while vigorous stirring going on. After about 10 minutes of continuous stirring at these conditions, the color of the solution changed to dark brown-black, showing formation of particles/ ink particles.

After the ink was synthesized (particulate dispersion in solvent), the particles were separated from the DI water by passing it through a filter paper and allowed to dry in a vacuum so as to remove any traces of the solvent. As the CZTS ink has to be deposited onto a substrate to be used in the solar photovoltaic applications, after its application onto the substrate, the proposed drying process for the inkjet printed samples is vacuum drying at 105 ºC for ~ 15 minutes. This will ensure complete removal of the base solvent, i.e. water in this case and also proper adhesion of the CZTS film to the substrate. An X-Ray Diffractometer (XRDynamic 500, Anton Paar) was used to perform X-ray diffraction studies on the produced powder after it had dried. To conduct additional measurements using ink powder, Raman spectrometer with an argon laser excitation source of wavelength 532 nm (Horiba LABRAM HR 800) was used. The ink particles were drop cast onto a glass substrate for doing UV-visible spectroscopy measurements (Perkin Elmer, LAMBDA 750) used to calculate the band gap using a Tauc plot. The particle dispersion was utilized for the particle size measurements (Zetasizer Nano ZSP, ZEN 5600). Multimode Scanning Probe Microscope (Bruker made) was used for the atomic force microscopy while, contact angle measurements were performed using KYOWA interface measurement and analysis system.

3. Results and discussion

The reducing agent supplied the electrons necessary for the cations in the bath to get reduced into their respective atoms, and it is speculated that as a result of intense swirling at 45 °C, the reduced atoms of copper, zinc, tin and sulphur organized themselves into a tetragonal crystal structure, forming CZTS crystals. As a result, the solution developed a brownish-black hue and had particles scattered throughout the solvent. There is also a possibility that other stable compounds also been formed along with unreacted metals.

3.1. X-ray diffraction studies

Fig. 1 shows the XRD pattern for CZTS ink particles. It can be observed that Cu_2ZnSnS_4 (JCPDS Card No. 00-026-0575) has an XRD pattern with peaks diffracted from the (211), (114), (220) and, (312) planes at $2\theta = 37.95°$, 40.56°, 46.92°, 56.46° respectively. This confirms the presence of tetragonal structure of CZTS (Kesterite) in the synthesized ink which has its tetragonal supercell derived from cubic zinc-blende lattice. The other possible compounds, such as, Cu_2S, SnS, ZnS, and unreacted metals coexist which is evident from the peaks observed at $2\theta = 24.72°$, 26.75°, 31.12°, 48.97°, 51.89° and 54.91° corresponding to the stable phases at room temperature, based on the standard values of provided data.

The presence of other prominent peaks, other than that for the CZTS, is due to the stable phases formed during the interaction of reduced ions due to vigorous stirring at 45 °C. If the temperature goes below 45 °C, the time taken by the solution to turn into ink (dark brownish-black colored particles) increases as the temperature goes on decreasing, while the XRD pattern hardly shows peaks corresponding to the CZTS.

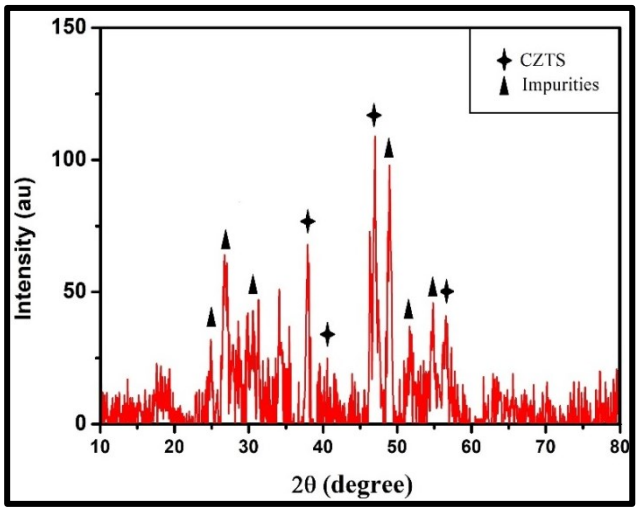

Fig. 1. XRD pattern for CZTS ink particles

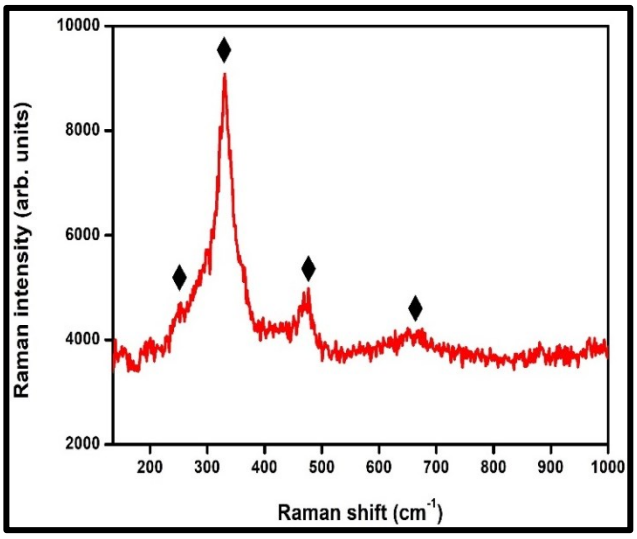

Fig. 2. Raman scattering spectra for CZTS Ink

Furthermore, the crystallite size was calculated using Debye–Scherrer formula:

$$d = \frac{0.94\,\lambda}{B\cos\theta} \quad (1)$$

where, d is the crystalline size, λ is the wavelength of CuKα radiation (k = 1.54 Å), B is the full width at half maximum (FWHM) value of the (220) peak, and θ is the Bragg angle. The calculated crystallite sizes came out to be 22.5 nm.

3.2. Raman spectroscopy analysis

The CZTS ink particles were drop-cast over a glass substrate for characterizing it for the Raman spectroscopy. The Raman spectra was obtained for the prepared ink at 532 nm excitation wavelength and is shown in Fig. 2. The strongest peak for CZTS in the Raman spectra can be observed at 336 cm^{-1}, which is in line with the literature [29]. Sharpness of the peaks indicates a high degree of crystallinity. Consequently, the existence of a distinct peak at 336 cm^{-1} suggests that the crystalline CZTS is present in the ink. The broad peak observed at 674 cm^{-1} may represent the blue-shifted peak of the second-order vibration of the CZTS. While, the presence of another prominent peak at 472 cm^{-1} and minor peak at 251 cm^{-1} signifies the presence of Cu_2S phase and other impurities respectively, again strengthening the observations form the XRD measurements.

The as-synthesized CZTS has very limited application due to the impurities. These impurities may act as a charge recombination sites, adversely affecting the power conversion efficiency of a solar cell.

3.3. Band gap measurements

Fig. 2 displays the Tauc plot i.e. a plot of $(\alpha h\upsilon)^2$ against the incident photon's energy for CZTS thin film. Utilizing Tauc's relation, as shown in equation 2, the bandgap of a semiconductor can be determined: where h is Planck's constant, υ is the incident photon frequency, and α is the absorption coefficient.

$$\alpha h\upsilon = \alpha_0 (h\upsilon - Eg)^n \quad (2)$$

Using the information from the absorption spectra acquired with the UV- Visible spectrophotometer, the bandgap of the produced thin film is 1.5 eV. The band gap in the CZTS crystal structure seen in Fig. 3 can range from 1.4 to 1.5 eV, depending on the concentrations of Tin and Zinc present in the CZTS crystal. The conclusions are in agreement with the literature [30] and shows the presence of Cu_2ZnSnS_4.

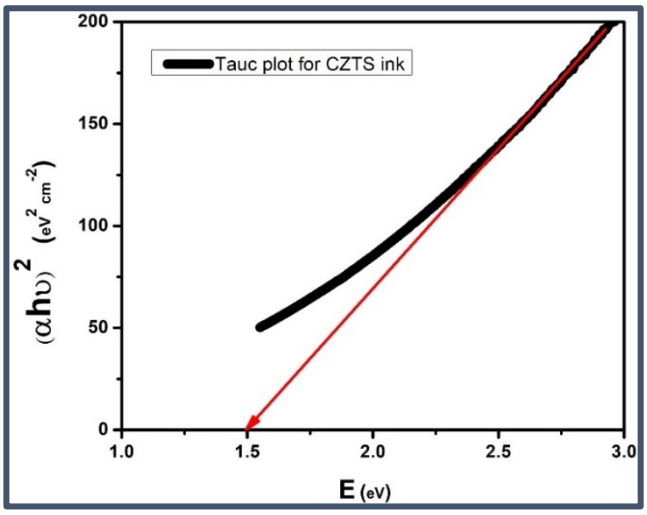

Fig. 3. Tauc plot for CZTS ink

3.4. Particle size distribution and measurements

Figs. 4 and 5 depicts the results of particle size distribution and measurements. As can be observed from Fig. 4, the particle size is broadly distributed in the range of 400 nm to 900 nm, with an average particle size of about 650 nm. Particle sizes smaller than 1000 nm (1µm) are generally desirable for the majority of inkjet printers to prevent ink particles from obstructing the nozzle's output. As a result, the acquired ink may be regarded as appropriate for its usage in an inkjet printer. As such, the ink preparation technique outlined above is suitable for producing printable CZTS ink.

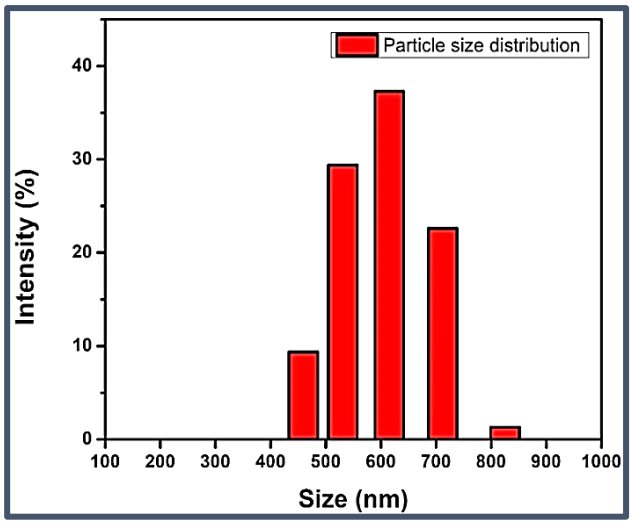

Fig. 4. Particle size distribution of CZTS ink

Atomic force microscopy (AFM) studies have been done on the prepared CZTS ink after 30 days of its preparations to check the effect of time for possible agglomeration of ink particles. After the said duration, the ink was subjected to ultrasonication for 10 minutes before its drop-casting over a glass substrate for the AFM measurements. Fig. 5 shows the AFM image (5 µm × 5 µm) of CZTS ink particles, and it can be observed that the particles hardly show any tendency for agglomeration and get readily separated due to ultrasonication treatment. Fig. 5 also shows that the size of the CZTS particles is less than 1 µm.

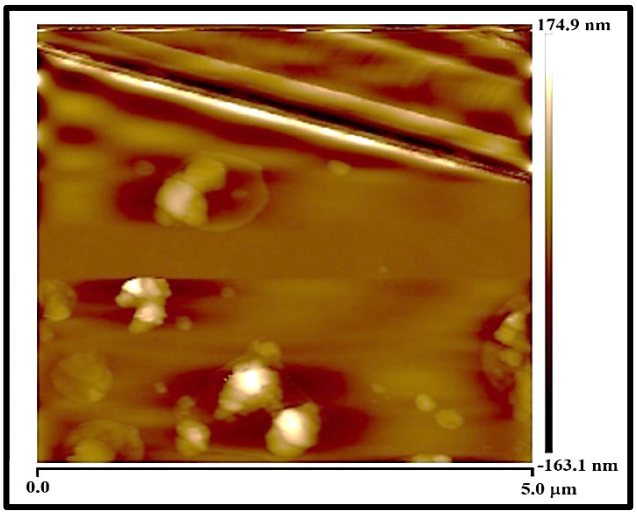

Fig. 5. AFM image (5 µm × 5 µm) of CZTS ink particles after 30 days of preparation (colour online)

3.5. Wettability and viscosity measurements

For getting optimum performance in terms of PCE and also to have a homogeneous coating, the contact angle of the ink or solution employed during manufacturing is essential. A contact angle between 10° and 30° is usually thought to be optimum [31]. This range encourages even wetting and spreading of the ink throughout the substrate, resulting in a thin layer that is consistent. The CZTS ink drop was put onto a glass substrate so as to measure the contact angle. From Fig. 6, it is evident that the water-based CZTS ink has a contact angle of 26.18 º, showing good wettability of the substrate by the ink.

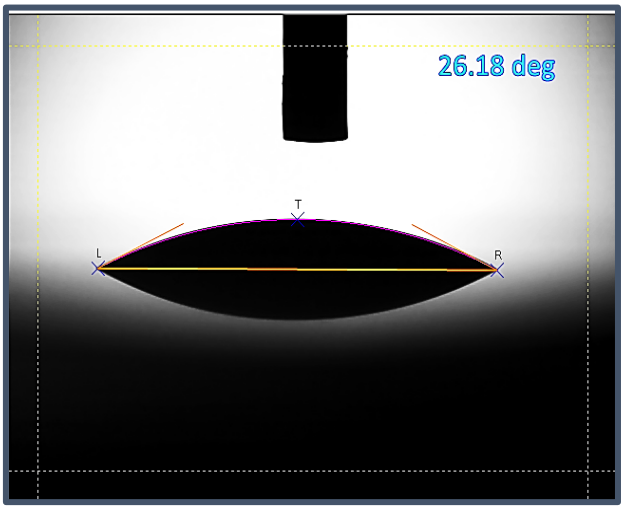

Fig. 6. Contact angle measurements of CZTS ink (colour online)

For ink-jet printing, a low viscosity (< 15 mPa s) ink has to be used in order to avoid clogging of the nozzle [32]. Viscosity on the other hand is dependent on

several factors, one of them is the shear rate. For the prepared water-based CZTS ink, it is found that for a shear rate greater than 1 /s, the viscosity falls below 15 mPa s.

4. Conclusion

For the first time, a vacuum-free and low-temperature method was developed for synthesizing water-based CZTS ink. An X-ray diffraction study confirmed the presence of CZTS along with some impurities as stable phases. Raman spectroscopy measurements backed the X-ray diffraction results. Using Tauc plot, a band gap of 1.5 eV was found for the synthesized ink derived using the UV-visible spectroscopic studies. Studies on particle sizes showed that the produced ink has particles ranging from 400 nm to 900 nm in size, have good wettability and appropriate viscosity making it suitable for ink-jet printing application. The compositional, morphological, and optical properties of the as-synthesized CZTS ink make it suitable for its use for inkjet printing and subsequent photovoltaic applications, while optimization of the amount of precursors, temperature, pH, and post-synthesis thermal treatments can be thought of a strategy to get phase-pure CZTS.

Acknowledgments

The authors acknowledge the support of the Department of Metallurgical and Materials Engineering, Malaviya National Institute of Technology Jaipur (MNIT Jaipur) and Materials Research Center (MRC), MNIT Jaipur for providing various facilities for the synthesis and characterizations. The authors acknowledge the XRD characterization support from the Department of Science and Technology, Government of India, under their FIST Program (sanction order no. SR/FST/ET-I/2021/857, dated 02/03/2022).

References

[1] S. Chu, A. Majumdar, Nature **488** (7411), 294 (2012).
[2] L. Vesce, Energies **16**(1), 425 (2023).
[3] T. Amrillah, Solar Energy **263**, 111982 (2023).
[4] Z. Q. Shi, D. Attygalle, A. H. Jayatissa, J. Mater. Sci.-Mater. Electron. **28**(2), 2290 (2017).
[5] N. S. Seroka, R. Taziwa, L. Khotseng, Materials **15**(15), 5338 (2022).
[6] S. Sivaraj, R. Rathanasamy, G. V. Kaliyannan, H. Panchal, A. J. Alrubaie, M. Jaber, Z Said, S. Memon, Energies **15**(22), 8688 (2022).
[7] W. A. Badawy, J. Adv. Res. **6**(2), 123 (2015).
[8] D. Saikia, A. Betal, J. Bera, S. Sahu, Mater. Sci. Semicond. Process. **150**, 106953 (2022).
[9] H. Katagiri, K. Jimbo, W. S. Maw, K. Oishi, M. Yamazaki, H. Araki, A. Takeuchi, Thin Solid Films **517**(7), 2455 (2009).
[10] X. Pan, X. Li, Y. Yang, C. Xiang, A. Xu, H. Liu, W. Yan, W. Huang, H. Xin, Adv. Energy Mater. **13**, 2301780 (2023).
[11] K. Rawat, K. Jha, G. Shishodia, P. Shishodia, J. Mater. Sci.-Mater. Electron. **34**, 1364 (2023).
[12] C. Yan, J. Huang, K. Sun, S. Johnston, Y. Zhang, H. Sun, A. Pu, M. He, F. Liu, K. Eder, L. Yang, Nat. Energy **3**, 764 (2018).
[13] S. Chander, S. K. Tripathi, I. Kaur, A. K. De, Mater. Today Sustain. **25**, 100662 (2024).
[14] K. Pal, P. Singh, A. Bhaduri, K. B. Thapa, Sol. Energy Mater. Sol. Cells **196**, 138 (2019).
[15] S. D. B. George, L. Narasimman, K. Nagarajan, R. R. Santhanaraj, D. Soren, J. J. Arockiasamy, P. Durai, S. Veeramani, J. Mater. Sci.-Mater. Electron. **35**(3), 1 (2024).
[16] P. K. Kannan, S. Chaudhari, S. R. Dey, Bull. Mater. Sci. **42**(1), 1 (2019).
[17] C. Y. Su, T. W. Kuo, P. C. Chen, Y. C. Chiu, P. C. Lin, C. C. Chang, Ceram. Int. **44**, S96 (2018).
[18] Y. P. Lin, Y. F. Chi, T. E. Hsieh, Y. C. Chen, K. P. Huang, J. Alloy Compd. **654**, 498 (2016).
[19] S. M. Bhosale, M. P. Suryawanshi, M. A. Gaikwad, P. N. Bhosale, J. H. Kim, A. V. Moholkar, Mater. Lett. **129**, 153 (2014).
[20] Y. H. Khattak, F. Baig, H. Toura, I. Harabi, S. Beg, B. M. Soucase, Appl. Surf. Sci. **497**, 143794 (2019).
[21] R. Sani, R. Manivannan, S. N. Victoria, Chalcogenide Lett. **14**(5), 165 (2017).
[22] M. Jiang, Y. Li, R. Dhakal, P. Thapaliya, M. Mastro, J. D. Caldwell, F. Kub, X. Yan, Photon. Energy **1**, 019501 (2011)
[23] P. Amrit, S. Jain, M. Tomar, V. Gupta, B. Joshi, Int. J. Appl. Ceram. Technol. **17**(3), 1194 (2020).
[24] D. Özbek, S. Erkan, M. Olgar, R. Zan, J. Alloys Compd. **1013**, 178514 (2025).
[25] H. Li, H. Shen, J. Zhang, J. Zheng, Y. Li, H. Bai, J. Chen, Z. Yue, L. Wang, J. Zeng, J. Alloy Compd. **995**, 174812 (2024).
[26] A. Wang, J. Huang, C. Yan, G. He, X. Cui, X. Yuan, S. Zhou, M. He, T. Qiu, C. Zhao, M. Green, K. Sun, X. Hao, Adv. Funct. Mater. **34**, 2407063 (2024).
[27] A. Wang, J. Cong, S. Zhou, J. Huang, J. Cao, X. Cui, X. Yuan, Y. Yao, Z. Xu, G. He, J. Liu, J. Cairney, Y. Chen, M. Green, S. Wei, K. Sun, X. Hao, Nat. Energy. **23**, 1 (2025).
[28] M. Albalawi, H. Bencherif, A. Ahmed, J. Electron. Mater. **53**, 7672 (2024).
[29] S. P. Ramkumar, G. Petretto, W. Chen, H. P. C. Miranda, X. Gonze, G. M. Rignanese, Phys. Rev. Mater. **6**(3), 035403 (2022).
[30] C. Malerba, F. Biccari, C. L. A. Ricardo, M. Valentini, R. Chierchia, M. Müller, A. Santoni, E. Esposito, P. Mangiapane, P. Scardi, A. J. Mittiga, J. Alloy Compd. **582**, 528 (2014).
[31] S. Ge, H. Gao, R. Hong, J. Li, Y. Mai, X. Lin, G. Yang, ChemSusChem **12**, 1692 (2019).
[32] D. Tobjörk, R. Österbacka, Adv. Mater. **23**, 1935 (2011).

*Corresponding author: kunal.meta@mnit.ac.in